2017 International Nuclear Atlantic Conference - INAC 2017
Belo Horizonte, MG, Brazil, October 22-27, 2017
ASSOCIAÇÃO BRASILEIRA DE ENERGIA NUCLEAR – ABEN

Agência Brasileira do ISBN
ISBN 978-85-99141-07-6
9 788599 141076

CFD ANALYSIS OF BLOCKAGE LENGTH ON A PARTIALLY BLOCKED FUEL ROD

Nikolas Lymberis Scuro[1], Gabriel Angelo[2], Edvaldo Angelo[3], Delvonei Alves de Andrade[1]

[1] Instituto de Pesquisas Energéticas e Nucleares (IPEN / CNEN - SP)
Centro de Engenharia Nuclear
Av. Professor Lineu Prestes 2242
05508-000 São Paulo, SP
nikolas.scuro@gmail.com ; delvonei@ipen.br

[2]Centro Universitário FEI
Departamento de Engenharia Mecânica
Av. Humberto de Alencar Castelo Branco, 3972-B
09850-901 São Paulo, SP
gangelo@fei.edu.br

[3]Universidade Presbiteriana Mackenzie
Escola da Engenharia – Grupo de Simulação Numérica
Rua da Consolação, 896 Prédio 6
01302-907 São Paulo, SP
eangelo@mackenzie.br

ABSTRACT

In LOCA accidents, fuel rods may balloon by the increasing of pressure difference between fuel rod and core vessel. With the balloon effect, the swelling can partially block the flow channel, affecting the coolability during reflood phase. In order to analyze the influence of blockage length after LOCA events, many numerical simulations using Ansys-CFX code have been done in steady state condition, characterizing the final phase of reflood. Peaks of temperature are observed in the middle of the fuel rod, followed by a temperature drop. This effect is justified by the increasing of heat transfer coefficient, originated from the high turbulence effects. Therefore, this paper considers a radial blockage of 90%, varying just the blockage length. This study observed that, for the same boundary conditions, the longer the blockage length originated after LOCA events, the higher are the central temperatures in the fuel rod.

1. INTRODUCTION

LOCA accidents in PWR nuclear reactors may affect the coolability of fuel assemblies. During this accident, fuel rods can overheat, accelerating the production of gases and solid products. With the high temperatures, the fission products increase the internal pressure of the fuel rod. It is known that during LOCA events, reactor vessel can be quickly depressurized. With both conditions, the fuel rod have a great pressure difference between internal and external boundaries. Thus, fuel rod can balloon, resulting in a radial and length deformation.

After the alarm of LOCA accident, the reactor scrams immediately. At the same time, emergency systems are responsible for coolability of the heat originated from radioactive decay. Among the available forms for emergency cooling, the injection of subcooled water is named reflood phase. It occurs from bottom to upper region of the reactor vessel.

Initially, the transient reflood phase is a two-phase flow due the high initial temperatures reached by fuel rods. However, after filling the reactor core with subcooled water, the temperatures drop slowly to reach the steady state with water-liquid phase.

There are many studies using thermo-hydraulic programs, in order to analyze the fuel rod behavior after LOCA accidents. One of them, [1] presents an experimental 7x7 assembly, heated electrically from a pseudo-cossenoinal function that, after reflood, it is possible to reach a safe steady-state after LOCA.

Using the program SEFLEX, [2] analyzed the behavior during reflood for two fuel rods. The first one with non-blockage and the second one partially blocked. The simulation used three different gases between fuel and the clad to analyze different thermal profiles. Due the number of results, it is possible to affirm that, the 90% partially blocked geometry presented highest peaks of temperatures when compared from a non-blockage geometry. Thus, these results showed a great security limit from the maximum designed to real applications.

A fluid-dynamic study, divided into three papers was accomplished to evaluate the influence of partially blocked channels for a 7x7 fuel assembly. For the first paper, [3] used a 4x4 blocked region with a quarter of total length as blocked length. Characterizing an LBLOCA (large break loss of coolant accident), the study showed large drops in velocity inside some blocked regions. For other channels, the flow could reach the steady-state form, which lead to an expressive increase of internal velocity, following by an abrupt drop, approximating the velocity to the initial condition.

For the second paper, [4] verified the influence of a 62% coplanar radial blockage, with a blockage length smaller than used in [3]. The results showed an average increasing of 25% in velocity when compared to the average velocity in non-blocked channels. An important result is the non-constant mass flow through blocked channels, reaching values 50% less than other normal channels.

For the last paper, [5] tested for a 62% non-coplanar blockage at the same conditions tested in [4] and have not found any different result, or, expressive change in fluid-dynamic behavior. All experiments were compared with the results of the thermo-hydraulic program COBRA [6], showing a good agreement with experimental data.

To simulate the influence of coolability inside partially blocked regions, [7] used many thermo-hydraulic programs. Among them, FEBA [8], SEFLEX [2], THETIS [9], ACHILLES [10], CEGB [11] and FLECHT-SEASET [12]. The main objective was to determine the blockage length limit for fuel rods after LOCA events. The results showed that, even with severe radial blockage (90%), with a blockage length minor than 100mm, these parameters could not affect directly the coolability of the fuel rod.

For blockage lengths longer than 150mm, with radial blockage greater than 80%, it was possible to observe that during reflood phase, high surface temperatures over cladding, could affect the reactor security. The study did not consider fuel relocation.

Fuel relocation during LBLOCA events can lead for a different heat generation at fuel rod. [13] Analyzed experimentally with a 5x5 assembly, with 3x3 partially blocked fuel rods, utilizing a cossenoinal function profile. The temperature peaks presented inside ballooned fuel rods were smaller when compared to a normal rod. As the ballooned region increased turbulence inside the flow channel, the increase of heat transfer coefficient, lead to minor temperatures. When the fuel relocation was considered, higher temperatures were observed when compared to normal fuel rods.

In order to analyze the influence of blockage length as the main factor in fuel rod coolability, [14] tested for a 90% radial blockage, for a 2x2 electrically heated two different blockage lengths. With constant mass flow inside blockage channels, the results indicated that,

independently from the geometry and reflood velocity used in the study, it is possible to reach a secure steady-state condition, but the time to reach it can be committed.

Computational fluid dynamics showed to be an excellent tool to obtain flow properties, as turbulence behavior and eddy dissipation. To validate all data, laser used in [15] and [16] and are one of the most modern alternatives.

As discussed, the reflood phase in PWR nuclear reactors contains a two-phase flow during initial conditions after emergency actions from LOCA prevention. Due to the numerous factors that can originate a LOCA event, it is very difficult to predict the ballooned resulting geometry.

Therefore, this study presents a numerical analysis utilizing the Ansys-CFX commercial code to evaluate the influence of the blockage length inside fuel rods. Using similar boundary conditions as in [14] the numerical simulations are responsible to capture the thermal gradient inside fuel rods, as well as the thermal behavior for the fluid inside the geometry, indicating the final condition after a reflood.

2. MODEL DEVELOPMENT

Numerical simulations based on a 2x2 assembly are designed inside a closed channel. For correct understanding the simulated geometry, Figure 1 shows the top view. The geometry is twice the size of a regular PWR fuel rod.

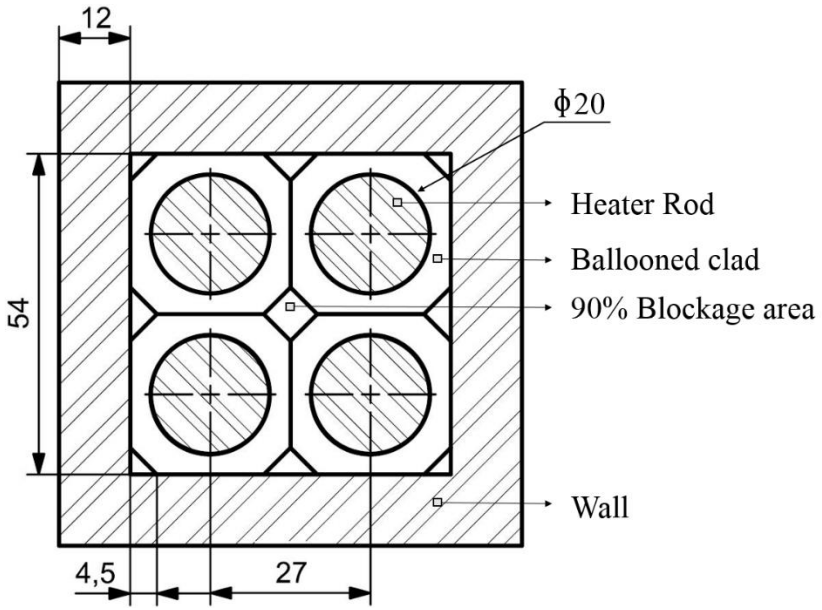

Figure 1: Top view of fuel rods

Fuel rods has 1800mm length, where, the ballooned region was constructed in the middle of the geometry. Both partially blocked regions are illustrated in Figure 2.

To study the influence of the blockage length, both geometries has the same total blockage length. Nevertheless, the long blockage length has twice the size of the 90% radial blockage.

Due to the lack of alignment with the objectives of this study, the spacer-grids were not included in the simulated geometry. As it is known from the study of [17], these elements require a great number of volumetric elements to correctly simulate its fluid-dynamics effects. Thereby, it is already possible to predict the pressure drop for each spacer-grids located in the fuel assembly.

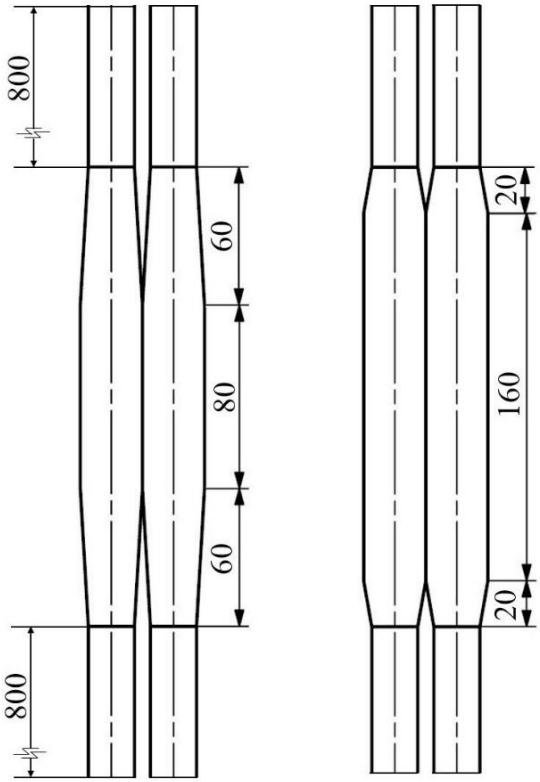

Figure 2: Short and long blockage geometries

For a correct understanding of the fluid-dynamic behavior, the fluid domain was added by 200mm at inlet and outlet region, totalizing a 2200mm fluid domain length.

3. CFD ANALYSIS OF FUEL ROD BUNDLE

The commercial code, Ansys-CFX, was utilized in the numerical simulations, where, all water properties were corrected by IAPWS (International Association for the Properties of Water and Steam) [18]. For the solid region, all properties from the commercial steel INCONEL® Alloy 600 was considered.

3.1. TURBULENCE MODEL: TWO EQUATIONS MODEL k-ε

In this study, the turbulence model k-ε were chosen due to its stability and computational time required for each simulation. Another factor is its major use in literature, [19]

Considering the Buossinesq's hypothesis Equation (1), the k-ε model includes two transport equations, so that, it can calculate the average Reynolds stress tensor. One for turbulent kinetic energy (k), shown in Equation (2) and turbulent dissipation (ε) presented in Equation (3).

$$-\rho\overline{u_i u_j} = \mu_t\left(\frac{\partial \bar{u}_i}{\partial x_j} + \frac{\partial \bar{u}_j}{\partial x_i} - \frac{2}{3}\frac{\partial \overline{u_k}}{\partial x_k}\delta_{ij}\right) - \frac{2}{3}\rho k\delta_{ij} \quad (1)$$

$$\frac{\partial}{\partial t}(\rho k) + \frac{\partial}{\partial x_i}(\rho k\overline{u_i}) = \frac{\partial}{\partial x_j}\left[\left(\mu + \frac{\mu_t}{\sigma_k}\right)\frac{\partial k}{\partial x_j}\right] + P_k + \rho\epsilon + \sqrt{\bar{S}_{ij}\bar{S}_{ij}} \quad (2)$$

$$\frac{\partial}{\partial t}(\rho\varepsilon) + \frac{\partial}{\partial x_i}(\rho\varepsilon\overline{u_i}) = \frac{\partial}{\partial x_j}\left[\left(\mu + \frac{\mu_t}{\sigma_\varepsilon}\right)\frac{\partial\varepsilon}{\partial x_j}\right] + C_{1\varepsilon}\frac{\varepsilon}{k}(P_k) - C_{2\varepsilon}\rho\frac{\varepsilon^2}{k} + \sqrt{\overline{S_{ij}}\,\overline{S_{ij}}} \quad (3)$$

As, P_k is the term of production of turbulent kinetic energy Equation. (4).

$$P_k = -\rho\overline{u'_i u'_j}\frac{\partial\overline{u_j}}{\partial x_i} \quad (4)$$

To equalize the number of incognitos with expressions utilized in the turbulence model, the relationship between the turbulent dynamic viscosity, turbulent kinetic energy and dissipation rate of turbulent kinetic energy is presented in Equation (5).

$$\mu_t = \frac{\rho C_\mu k^2}{\varepsilon} \quad (5)$$

Constant values for this turbulence model, $C_{1\varepsilon}$, $C_{2\varepsilon}$, C_μ, σ_k, σ_ε are respectively equal to 1.44 , 1.92 , 0.09 , 1.0 and 1.3.

4. COMPUTATIONAL DOMAIN

The computational domain was considered bi-symmetric at *xz* and *yz* planes due to the reduction in volumetric elements necessary to obtain a correct numeric simulation.

Figure 3 shows the principal regions in the computational domain, among them: (i) fluid domain, (ii) inlet, (iii) outlet, (iv) solid domain (v) ballooned region and other boundary conditions.

Using the methodology proposed by [20], where, increasing the number of elements by an iteration method, using the same boundary conditions, the resultant error tends to an infinitesimal variation when compared to the previously iteration. Thus, the numerical solution is independent from the mesh.

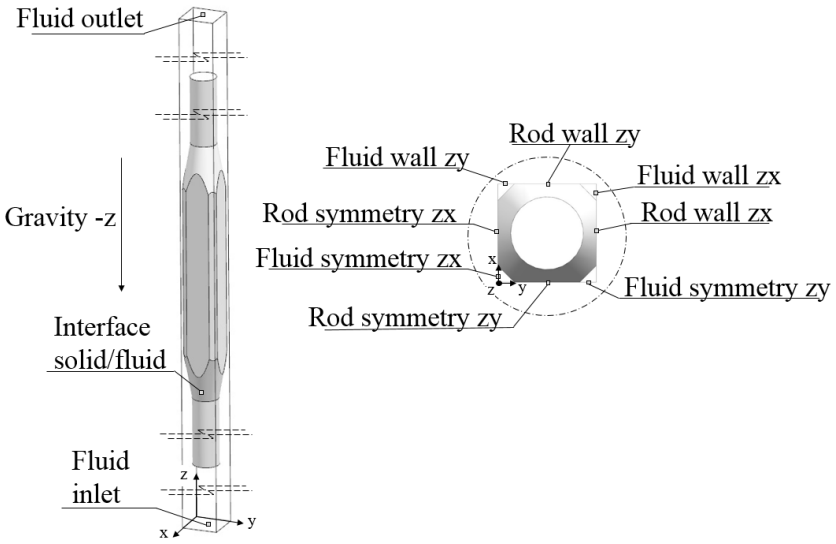

Figure 3: Isometric view of principal regions and boundary conditions

To verify the numerical convergence for the fluid domain separately, the density difference between inlet and outlet domain was compared to the IAPWS table [18]. For the solid domain, one geometric point was created and named as “Thermocouple”, to illustrate how the same point vary the temperature during convergence.

Figure 4 shows the numerical convergence for the computational domain with three main physical properties. The Total Heat Power is the heat transferred to the fluid domain. This property is capable to show the equilibrium of, inlet density, velocity, specific heat at constant pressure and temperature difference beyond inlet and outlet.

All the presented data is illustrated in Figure 4 as a function of the number of elements. The dotted line shows the point in which the simulation reaches the equilibrium used in this paper.

As this study considers the heat transfer through the fluid beyond heat generation by solid domain, both have different values for the ideal number of elements. Figure 4 already shows these relations for both domains with the final mesh for each situation of the convergence.

For the final explanation for the numerical convergence, all data illustrated in Figure 4 shows the results for the minor inlet velocity and all geometries due to the lowest buoyancy forces. The other boundary conditions converged with the same number of elements.

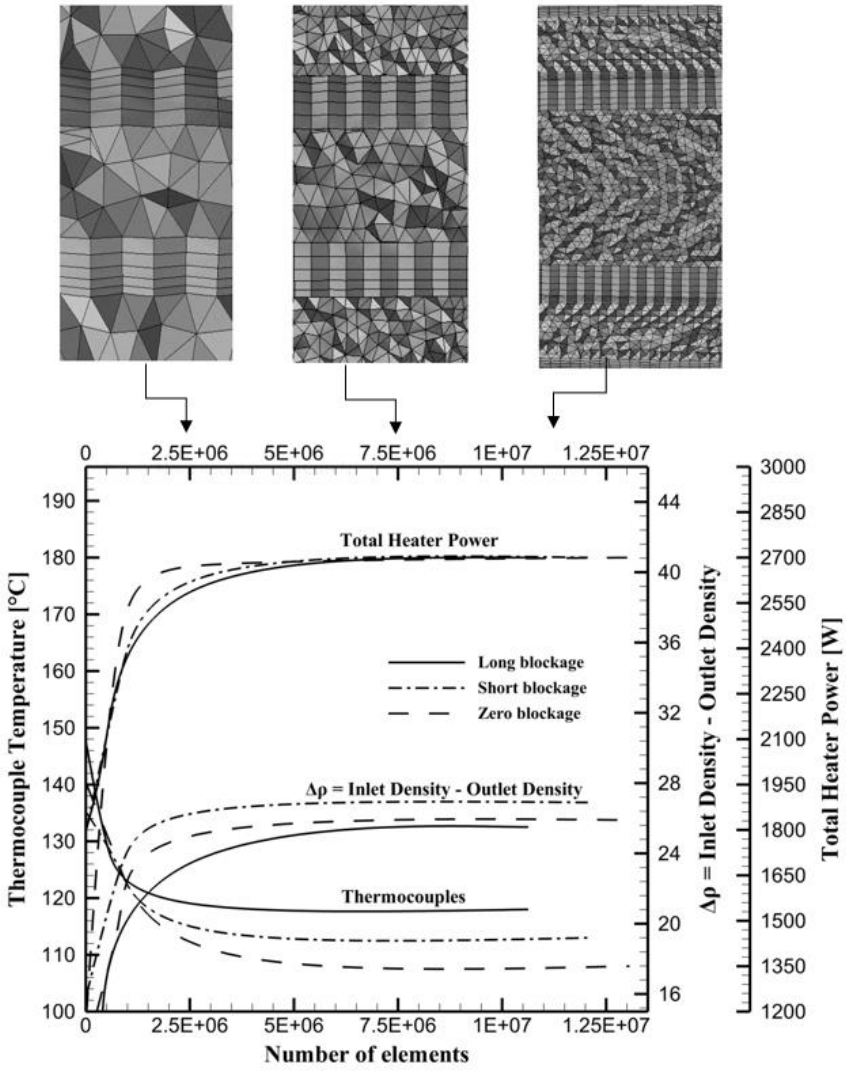

Figure 4: Numerical convergence for all geometries simulated using 2cm/s as inlet velocity

5.BOUNDARY CONDITIONS

All boundary conditions were divided for each computational domain, one for the solid domain, other for the fluid domain.

For the fluid domain:
(i) Inlet velocity (2cm/s, 2.5cm/s and 3.5cm/s)
(ii) Constant inlet temperature (50°C)
(iii) Outlet (1 atm - Absolute pressure)
(iv) Symmetry walls
(v) Smooth walls
(vi) Gravity at –z
(vii) Interface fluid/solid with heat transfer

For the solid domain:
(viii) Interface solid/fluid with heat transfer
(ix) Symmetry walls
(x) Rod walls
(xi) Smooth walls
(xii) Subdomain for linear heat generation

The use of gravity at *–z* lead to a correct calculation for buoyancy forces. So that, numerical simulation occurs considering real orientation for fuel rods.

5.1. CONVERGENCE CRITERIA

The mathematical model used a convergence criteria with error lower than 10^{-5} for root mean square (RMS) for the mass, momentum and energy.

6. RESULTS

6.1. VELOCITY ALONG FUEL ROD

To observe all fluid dynamics behavior originated by partially blocked effect, the velocity profile illustrated at the Figures 5-7 pass through radial blockage, located on the center of the real geometry (Figure 1).

Figure 5 illustrate the velocity profile for the non-blocked geometries, for all inlet velocities used during simulations. Up to 200mm, the velocity presented is the region of fluid domain without fuel rod. When the fluid enter in contact with fuel rod, the cross sectional area is reduced, and the velocity is increased. The same behavior occurs at the outlet.

For the same region with short and long blockage, all data are illustrated, respectively at Figure 6 and Figure 7. A distinct behavior was observed due the 90% radial blockage. The flow area is great reduced, creating a zone of high velocity when compared to non-blockage fuel rod.

For the short blockage (Figure 6), a velocity peak observed at 1100mm follows a drop. An unstable region appeared between 1500mm to 2000mm.

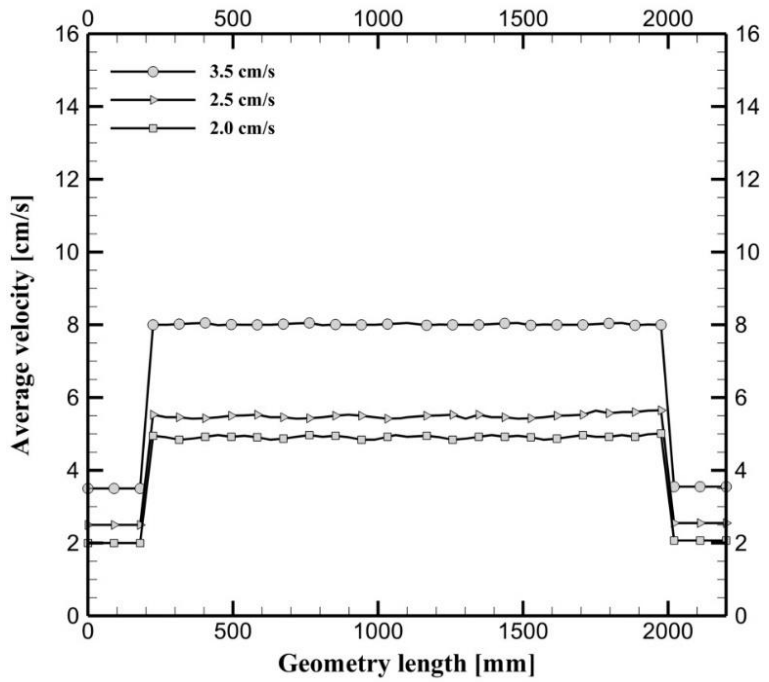

Figure 5: Average velocity for zero blockage

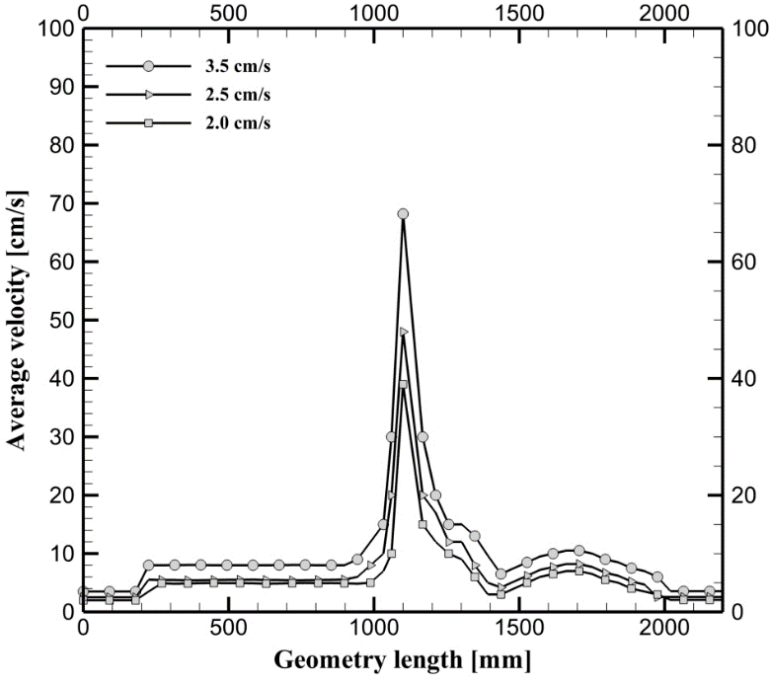

Figure 6: Average velocity for short blockage

A similar behavior was verified for long-blockage (Figure 7), but, due to the size of the blockage length, the boundary layer was completely evolved and created greater velocities peaks, following by an abruptly drop. This effect create the same unstable region observed in the short-blockage, but with higher intensity. Furthermore, as the velocity peak was higher

when compared to short-blockage, the property was maintained for a longer length, what influenced wall heat transfer coefficient. This issue will be discussed in the next topics.

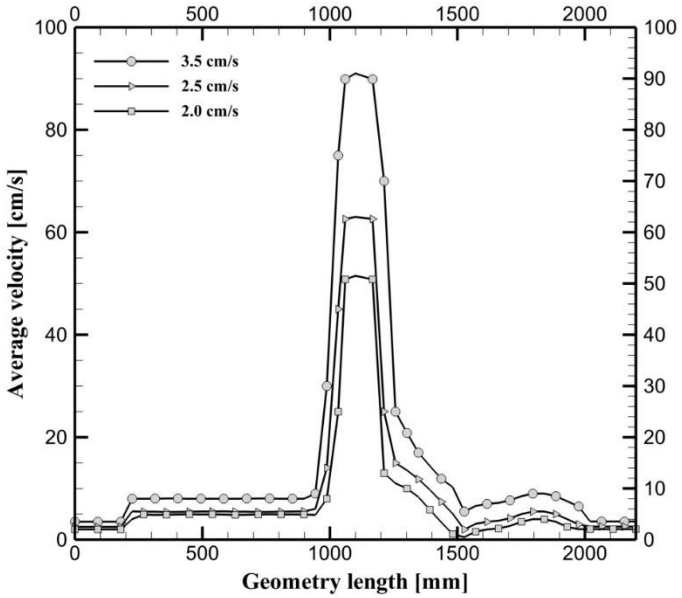

Figure 7: Average velocity for long blockage

6.2 FUEL ROD TEMPERATURE PROFILES

For nuclear power reactors, the center of the fuel rods contemplates the highest temperatures. To analyze all thermo-hydraulic behavior originated by partially blocked effect, all temperature profiles are illustrated at Figure 8, Figure 9 and Figure 10. The inlet velocity used was respectively 2cm/s, 2.5cm/s and 3.5cm/s.

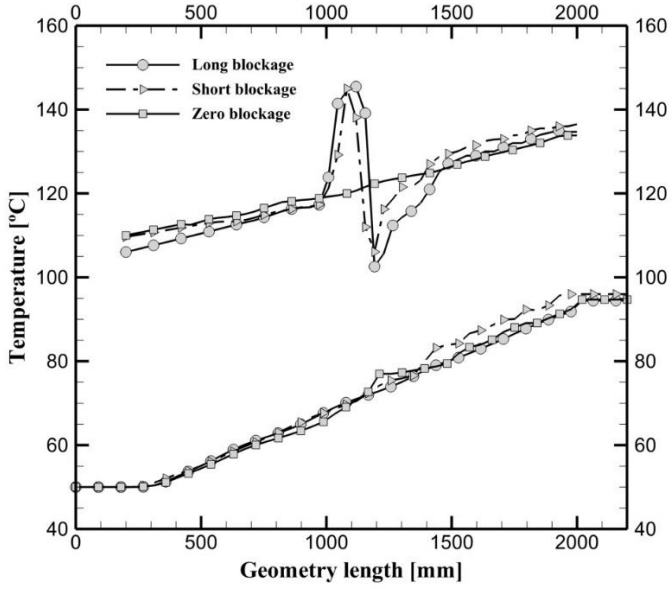

Figure 8: Thermal behavior for solid/fluid with 2cm/s

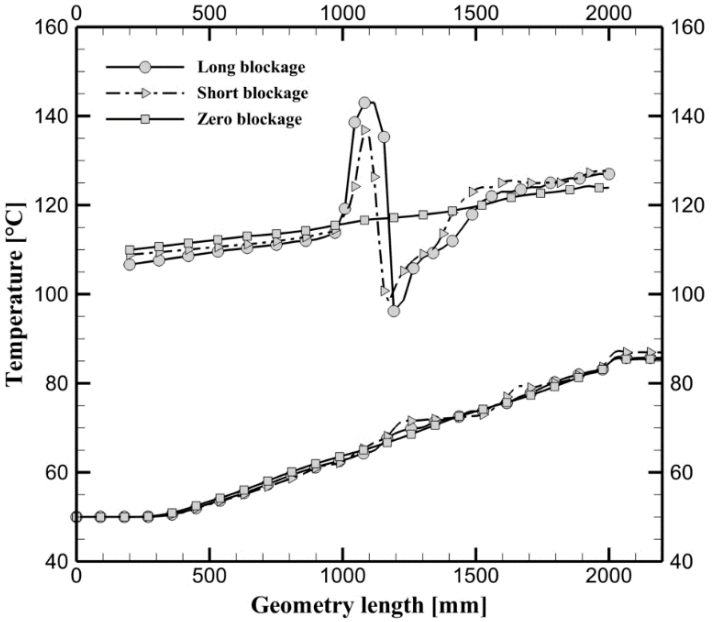

Figure 9: Thermal behavior for solid/fluid with 2.5 cm/s

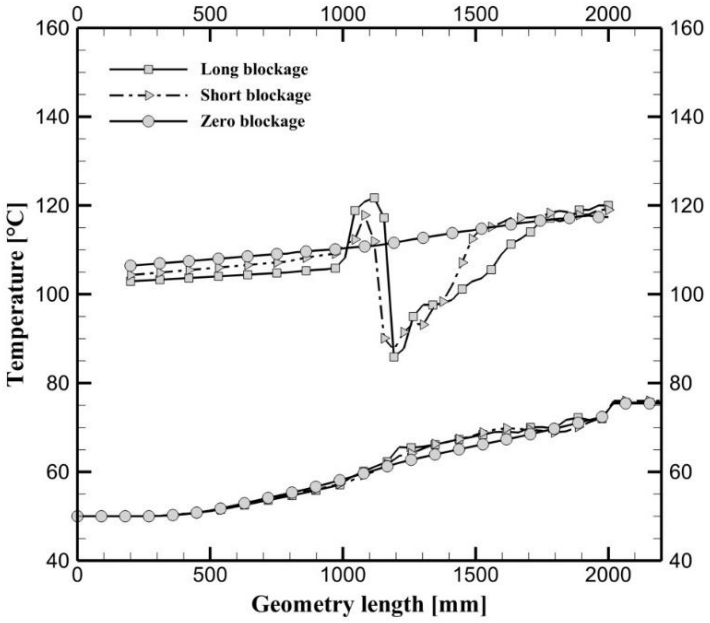

Figure 10: Thermal behavior for solid/fluid with 3.5 cm/s

It is possible to observe that, regardless of inlet velocity, all non-blocked conditions showed a linear and gradual heating along the length. This result is reasonable for the linear heat generation.

For the partially blocked geometries, a temperature peak is observed exactly at the ballooned region (1000mm to 1200mm). The maximum value for temperature did not show great variations between 2cm/s and 2.5cm/s, but when it reaches 3.5cm/s, the highest point

drops substantially. To present all data obtained, Table 1 shows all temperature peaks in the center of the computational domain.

Table 1: Temperature Peaks for all geometries

	2 cm/s	2.5 cm/s	3.5 cm/s
Zero-blockage	120.3 °C	116.8 °C	110.8 °C
Short-blockage	145.0 °C	136.9 °C	117.8 °C
Long-blockage	145.5 °C	143.0 °C	121.7 °C

When non-blockage conditions are compared to partially blocked temperature peaks, it is observed that the greater the blockage length, the greater the center temperature. This effect may be lesser relevant when compared to a higher inlet velocity, as the turbulent effect becomes more evident. Another perceptible effect originated by ballooned effect, is a drop in the temperature locating its minimum value at 1200mm. Table 2 shows all minimum temperatures for the respective location.

Table 2: Minimum central temperatures for all geometries.

	2 cm/s	2.5 cm/s	3.5 cm/s
Zero-blockage	123.4 °C	117.2 °C	111.6 °C
Short-blockage	106.0 °C	100.8 °C	87.5 °C
Long-blockage	102.6 °C	96.2 °C	85.5 °C

One of the reasons to originate a drop in temperature is the high turbulence effects originated by ballooned region. Figure 10 shows streamlines for 3.5 cm/s for all geometries.

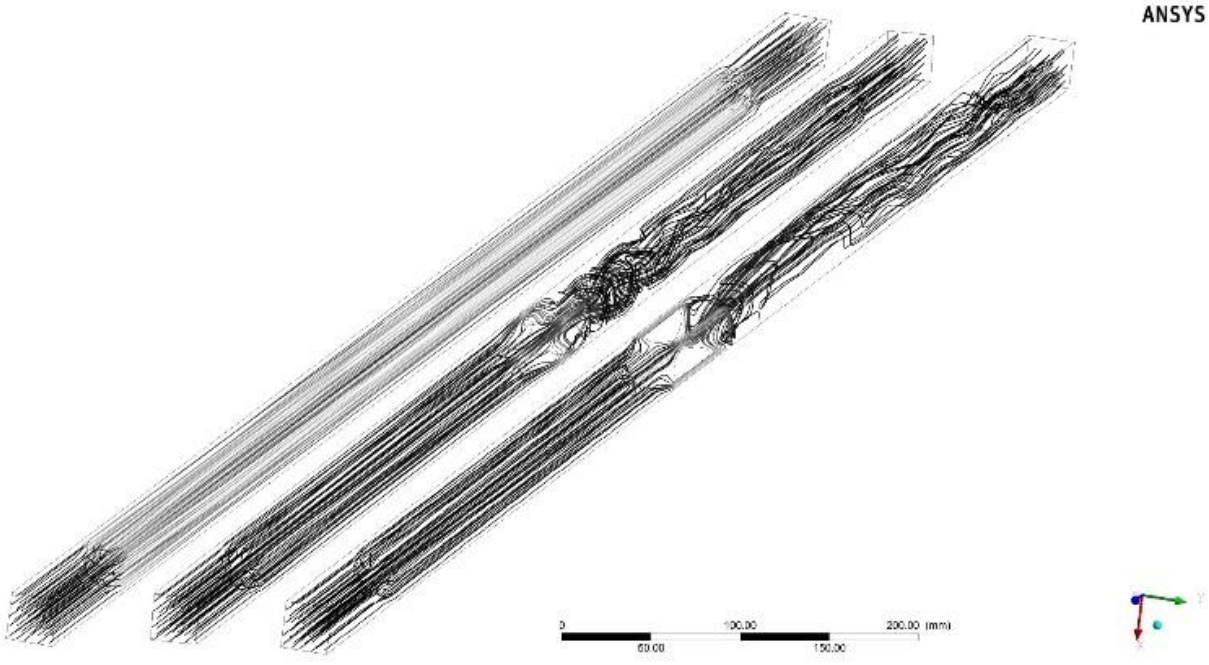

Figure 11: Streamlines for 3.5 cm/s for all geometries

Along fluid flow, the turbulence becomes regular and the fuel rod temperatures become next to non-blockage conditions. To understand how turbulence influenced wall heat transfer coefficient, Figure 12 shows for long blockage the respective property at 3.5cm/s.

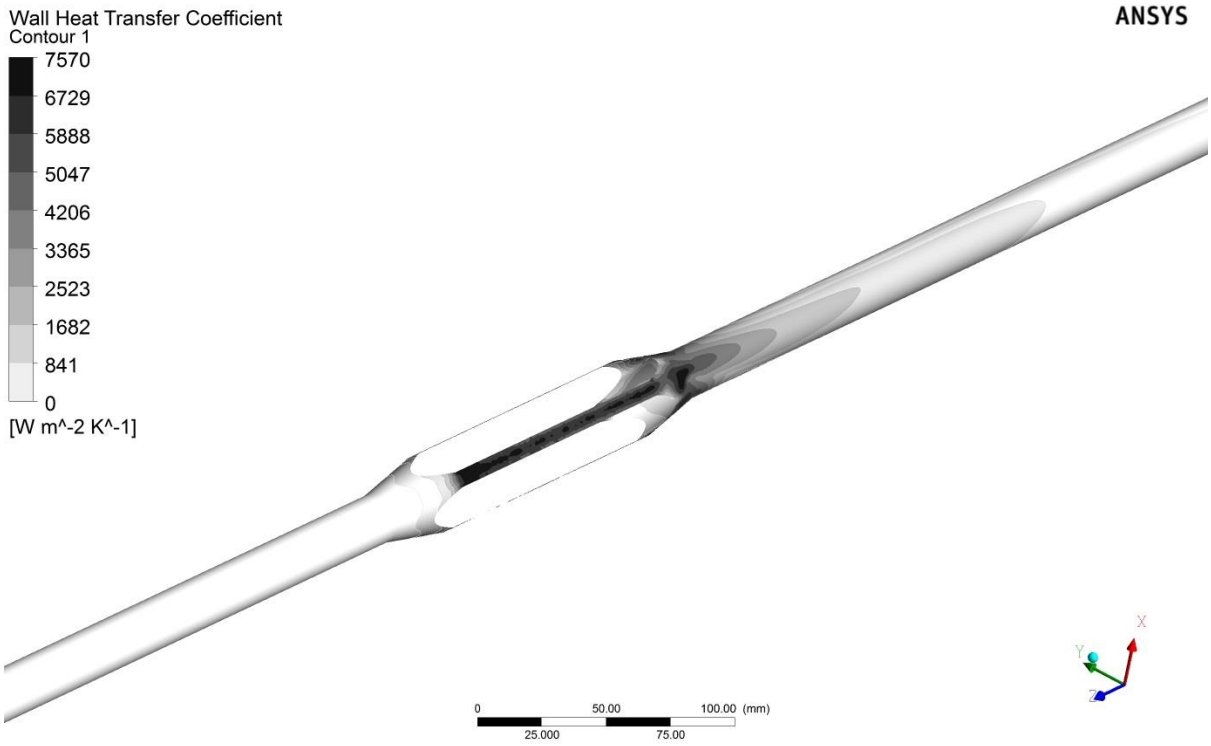

Figure 12: Wall heat transfer coefficient for long blockage (3.5cm/s)

Therefore, even with high wall heat transfer coefficient inside ballooned area a presence of high temperatures just reduces its magnitude when inlet velocity is increased.

CONCLUSIONS

After LOCA events, fuel rods may balloon, when this strain occurs, velocity, temperature and turbulence for each fuel rod vary according to radial and blockage-length.

All partially blocked geometries have a significant increasing on central region of the rod temperature. The smaller the inlet velocity, the greater the outlet fluid temperature. For the critical situation (inlet velocity at 2 cm/s), the increasing on temperature reached 22% when compared to the same non-blocked condition.

The turbulence increased heat transfer capacity, so that, fuel rod temperatures dropped after passing through the ballooned region, reaching regular values after some length (Figure 11, Figure 12 and Figure 13).

The velocity profiles encountered are similar to analogous studies of [7], however, with the use of CFD, flow properties could be better observed as pointed by [3]–[5]

It is important to reinforce that mass flow is considered constant for this numeric simulation. For a simulation with many fuel rods, mass flow could pass around the ballooned regions to maintain pressure drop constant. It could increase even more the peak of temperatures [21], [3], [8] and [22].

It is not possible to compare quantitatively all data obtained during simulations to another studies, but, as discussed, the qualitative results were very satisfactory. The agreement with other studies reinforce that the peaks of temperature originated by ballooned effect are more dangerous when compared to the temperature drop caused by turbulence.

A more complex study is under progress. The aim is to study the effects of natural circulation for ballooned fuel rods, and how the velocity, originated by heat decay, influences the temperature profile along the fuel rod.

ACKNOWLEDGMENTS

The authors would like to acknowledge Nuclear and Energy Research Institute, IPEN-CNEN/SP for the infrastructure, particularly the computer laboratory.

REFERENCES

[1] M. Naitoh, K. Chino, and H. Ogasawara, "Cooling mechanism during transient reflooding of a reactor fuel bundle after loss of coolant," *Nucl. Eng. Des.*, vol. 44, no. 2, pp. 193–200, Nov. 1977.

[2] P. Ihle and K. Rust, "PWR reflood experiments using full length bundles of rods with zircaloy claddings and alumina pellets," *Nucl. Eng. Des.*, vol. 99, pp. 223–237, Feb. 1987.

[3] M. L. Ang, A. Aytekin, and A. H. Fox, "Analysis of flow distribution a PWR fuel rod bundle model containng A 90% blockage," *Nucl. Eng. Des.*, vol. 103, no. 2, pp. 165–188, Aug. 1987.

[4] M. L. Ang, A. Aytekin, and A. H. Fox, "Analysis of flow distribution in a PWR fuel rod bundle model containing a blockage - Part 1. A 61% coplanar blockage," *Nucl. Eng. Des.*, vol. 108, no. 3, pp. 275–294, Jul. 1988.

[5] M. L. Ang, A. Aytekin, and A. H. Fox, "Analysis of flow distribution in a PWR fuel rod bundle model containing a blockage - Part 2. A non-coplanar blockage," *Nucl. Eng. Des.*, vol. 108, no. 3, pp. 295–314, Jul. 1988.

[6] K. R. Thurgood, M. J.; Kelly, J. M.; Guidotti, T. E.; Kohrt, R. J.; Crowell, "COBRA/TRAC-A thermal-hydraulics code for transient analysis of nuclear reactor vessels and primary coolant systems.," *Comm.*, 1983.

[7] C. Grandjean, "Coolability of blocked regions in a rod bundle after ballooning under LOCA conditions," *Nucl. Eng. Des.*, vol. 237, no. 15–17, pp. 1872–1886, Sep. 2007.

[8] K. Ihle, P.; Rust, "FEBA-flooding experiments with blocked arrays-influence of blockage shape," *Trans. Am. Nucl. Soc.*, 1979.

[9] K. G. Jowitt, D.; Cooper, C. A., ; Pearson, "The THETIS 80% blocked cluster experiment. Part 5," *UKAEA At. Energy Establ.*, vol. No. AEEW-R, 1984.

[10] K. G. Denham, M. K.; Jowitt, D.; Pearson, "ACHILLES unballooned cluster experiments, part 1, description of the ACHILLES rig, test section and experimental procedures.," *AEEW-R2326.*, 1989.

[11] B. D. G. Fairbairn, S. A. ; Piggott, "Flow and Heat Transfer in PWR Rod Bundles in the Presence of Blockage due to clad Ballooning; Experimental Data Report-Part 2," *CEGB Rep. TPRD/B/0458*, vol. 2, 1984.

[12] L. E. Hochreiter, "FLECHT SEASET program. Final report," *Westinghouse Electr. Corp., Pittsburgh, PA*, vol. No. NUREG/, no. Westinghouse Electric Corp., Pittsburgh, PA (USA), 1985.

[13] B. J. Kim, J. Kim, K. Kim, S. W. Bae, and S.-K. Moon, "Effects of fuel relocation on reflood in a partially-blocked rod bundle," *Nucl. Eng. Des.*, vol. 312, pp. 239–247, 2017.
[14] K. Kim, B.-J. Kim, H.-S. Choi, S.-K. Moon, and C.-H. Song, "Effect of a blockage length on the coolability during reflood in a 2×2 rod bundle with a 90% partially blocked region," *Nucl. Eng. Des.*, vol. 312, pp. 248–255, 2017.
[15] E. E. Dominguez-Ontiveros, Y. A. Hassan, M. E. Conner, and Z. Karoutas, "Experimental benchmark data for PWR rod bundle with spacer-grids," *Nucl. Eng. Des.*, vol. 253, pp. 396–405, Dec. 2012.
[16] E. E. Dominguez-Ontiveros and Y. A. Hassan, "Non-intrusive experimental investigation of flow behavior inside a 5×5 rod bundle with spacer grids using PIV and MIR," *Nucl. Eng. Des.*, vol. 239, no. 5, pp. 888–898, May 2009.
[17] S. Cheng, H. Chen, and X. Zhang, "CFD analysis of flow field in a 5×5 rod bundle with multi-grid," *Ann. Nucl. Energy*, vol. 99, pp. 464–470, 2017.
[18] H. J. Wagner, W.; Kretzschmar, "IAPWS industrial formulation 1997 for the thermodynamic properties of water and steam," *Int. Steam Tables Prop. Water Steam Based Ind. Formul. IAPWS-IF97*, p. 7–150., 2008.
[19] B. E. Launder and D. B. Spalding, "The numerical computation of turbulent flows," *Comput. Methods Appl. Mech. Eng.*, vol. 3, no. 2, pp. 269–289, Mar. 1974.
[20] E. G. Stern, F.;Wilson, R. V.; Coleman, H. W.; Paterson, "Comprehensive approach to verification and validation of CFD simulations-Part 1: methodology and procedures," *Trans. Soc. Mech. Eng. J. Fluids Eng.*, vol. 123(4), pp. 793–802, 2001.
[21] K. Ihle, P.; Rust, "SEFLEX fuel rod simulator effects in flooding experiments. Pt. 3," *Kernforschungszentrum Karlsruhe GmbH*, 1986.
[22] E. Dominguez-Ontiveros and Y. A. Hassan, "Experimental study of a simplified 3x3 rod bundle using DPTV," *Nucl. Eng. Des.*, vol. 279, pp. 50–59, Nov. 2014.